



Modelling the transport phenomena and texture changes of chicken breast meat during the roasting in a convective oven

Rabeler, Felix; Feyissa, Aberham Hailu

Published in:
Journal of Food Engineering

Link to article, DOI:
[10.1016/j.jfoodeng.2018.05.021](https://doi.org/10.1016/j.jfoodeng.2018.05.021)

Publication date:
2018

Document Version
Peer reviewed version

[Link back to DTU Orbit](#)

Citation (APA):
Rabeler, F., & Feyissa, A. H. (2018). Modelling the transport phenomena and texture changes of chicken breast meat during the roasting in a convective oven. *Journal of Food Engineering*, 237, 60-68.
<https://doi.org/10.1016/j.jfoodeng.2018.05.021>

General rights

Copyright and moral rights for the publications made accessible in the public portal are retained by the authors and/or other copyright owners and it is a condition of accessing publications that users recognise and abide by the legal requirements associated with these rights.

- Users may download and print one copy of any publication from the public portal for the purpose of private study or research.
- You may not further distribute the material or use it for any profit-making activity or commercial gain
- You may freely distribute the URL identifying the publication in the public portal

If you believe that this document breaches copyright please contact us providing details, and we will remove access to the work immediately and investigate your claim.

1 **Modelling the transport phenomena and texture changes of chicken breast meat during the**
2 **roasting in a convective oven**

3

4 **Felix Rabeler , Aberham Hailu Feyissa***

5 Food Production Engineering, National Food Institute, Technical University of Denmark (DTU),
6 Denmark

7 *Corresponding author:

8 Søtofts Plads, 2800, Kgs. Lyngby, Denmark

9 Email address: abhfe@food.dtu.dk, Tel.: +45 45252531

10

11

12 Keywords: COMSOL Multiphysics, heat and mass transfer, poultry meat, quality prediction,
13 thermal processing, transport in porous media

14

15 **Abstract**

16 A numerical 3D model of coupled transport phenomena and texture changes during the roasting
17 of chicken breast meat in a convection oven was developed. The model is based on heat and mass
18 transfer coupled with the kinetics of temperature induced texture changes of chicken breast meat.

19 The partial differential equations of heat and mass transfer as well as the ordinary differential
20 equations that describe the kinetics of the texture changes were solved using COMSOL

21 Multiphysics® 5.2a. The predicted temperature, moisture and texture (hardness, chewiness and
22 gumminess) profiles were validated using experimentally values. The developed model enables
23 the prediction of the texture development inside the chicken meat as function of the process

24 parameters. The model predictions and measured values show the clear effect of changing
25 process settings on the texture profiles during the roasting process. Overall, the developed model
26 provides deep insights into the local and spatial texture changes of chicken breast meat during the
27 roasting process that cannot be gained by experimentation alone.

28 **1. Introduction**

29 Heat treatment of chicken breast meat is a crucial processing step in households, professional
30 kitchens and large-scale food industries to achieve a safe and high quality product. Roasting of
31 chicken meat in a convection oven is a common process that involves simultaneous heat and
32 mass transfer. However, the roasting affects the microstructure (Feyissa et al., 2013;
33 Wattanachant et al., 2005), texture (Wattanachant et al., 2005) and appearance (Fletcher et al.,
34 2000) of the product and, consequently, its acceptance by the consumer.

35 The texture of the chicken meat is the highest rated quality attribute for the consumer during
36 consumption (Lawrie and Ledward, 2006) and it is mainly influenced by protein denaturation
37 which leads to fiber shrinkage and straightening (Tornberg, 2005; Wattanachant et al., 2005).
38 Consequently, the microstructure is becoming denser with compact fiber arrangements which
39 results in the toughening of the chicken meat during the heating (Christensen et al., 2000; Lewis
40 and Purslow, 1989; Wattanachant et al., 2005). Moreover, the protein denaturation leads to a
41 reduction of the water holding capacity (WHC) of the chicken breast meat. The unbound water
42 migrates into the spaces between the meat fibers which leads to a toughening of the meat and to
43 the loss of water during the roasting process (Micklander et al., 2002; Tornberg, 2005).

44 The quality of the final product is mainly controlled by the chef or operator through adjustments
45 of the process settings. However, this is still based on the cook-and-look approach, which relies
46 on the experience and skills of the chef or operator. A number of researchers measured

47 experimentally the texture change of poultry meat with temperature (Barbanti and Pasquini,
48 2005; Wattanachant et al., 2005; Zell et al., 2010) and Rabeler and Feyissa (2017, submitted for
49 publication) developed kinetic models to describe these changes with time. However, to gain the
50 relationship between the process conditions and the texture development inside the chicken meat,
51 the spatial temperature and time history during the roasting process is needed.

52 Mechanistic models of heat and mass transfer (based on fundamental physical laws) are able to
53 predict the temperature and moisture distribution during the cooking process of meat (Feyissa et
54 al., 2013; van der Sman, 2007), beef meat (Kondjoyan et al., 2013; Obuz et al., 2002) or poultry
55 meat (Chang et al., 1998; van der Sman, 2013). However, for the roasting of chicken breast meat
56 only a limited number of mathematical models are available.

57 Chen et al. (1999) developed a model of heat and mass transfer for convection cooking of
58 chicken patties. In their model they described the transport of moisture inside the chicken patties
59 by diffusion, which is a common approach for modelling mass transfer (Huang and Mittal, 1995;
60 Isleroglu and Kaymak-Ertekin, 2016; Kassama et al., 2014). However, the moisture transport
61 during the cooking process cannot be explained adequately by pure diffusion models (Feyissa et
62 al., 2013; van der Sman, 2007). Roasting of chicken breast meat leads to protein denaturation, the
63 shrinkage of the protein network and the reduction of the water holding capacity. This induces a
64 pressure gradient inside the meat and the expulsion of the excess moisture to the surface of the
65 meat.

66 This approach was used by van der Sman (2013) to model the cooking of chicken breast meat in
67 an industrial tunnel oven. The author showed that the model is able to predict the temperature and
68 moisture development inside the chicken meat for cooking temperatures below the boiling point.
69 However, the presented cooking temperatures (45 to 100 °C) and times (up to 160 min) are not

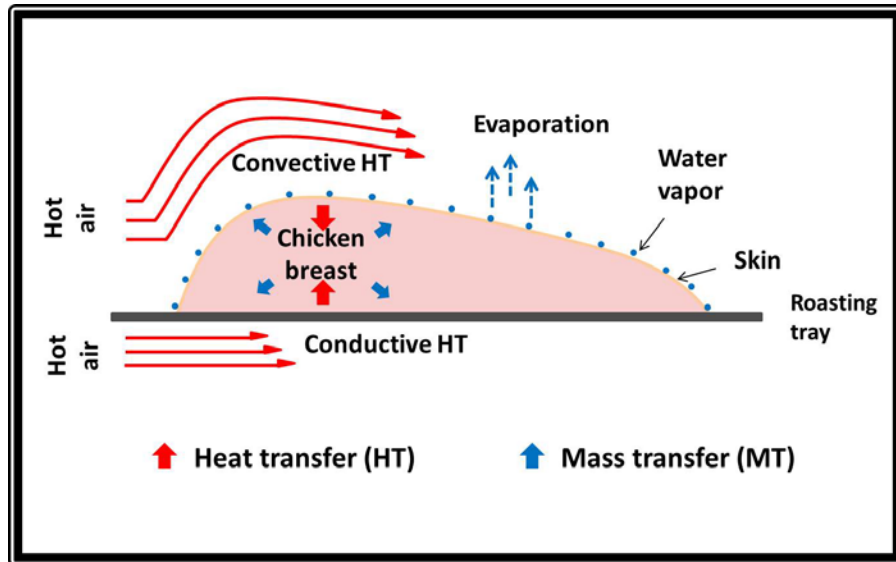
70 common settings for the roasting of chicken meat in industrial convection ovens, where hot dry
71 air with more than 150 °C is employed (Chen et al., 1999; Guerrero-Legarreta and Hui, 2010).
72 Thussu and Datta (2012) showed that by coupling texture kinetics with physical based models of
73 heat and mass transfer, the texture development during the frying of potato stripes can be
74 predicted. However, for chicken breast meat or other muscle foods no attempt was made to
75 couple kinetic models for textural changes with mechanistic models of heat and mass transfer to
76 predict the local and spatial texture changes.
77 Therefore, the aim of this study is to first develop a mechanistic model to predict the temperature
78 and moisture profiles of chicken breast meat during the roasting in a convection oven. Our
79 hypothesis is then that by coupling the developed model for heat and mass transfer with the
80 kinetic models of heat induced textural changes for chicken meat, the texture profile during the
81 roasting process can be predicted as function of process parameters. Afterwards, the model
82 predictions will be validated against experimental values.

83 **2. Modelling of transport phenomena and texture changes**

84 **2.1. Process description and model formulation**

85 Roasting in a convection oven is a thermal process, where the product is heated at high
86 temperatures (150 - 300 °C) by circulated hot air. The main mechanisms during the roasting of
87 chicken breast meat in a convective oven are illustrated in Fig. 1. Heat is transferred mainly
88 through convection from the surrounding circulated hot air while a conductive heat flux comes
89 from the roasting tray (bottom of chicken breast). The surrounding oven walls are made of
90 polished stainless steel, thus, the effect of radiation is small compared to the convective transport
91 (see section 3.2.1) (Feyissa et al., 2013). The effect of radiation was included in the model by
92 using an estimated effective heat transfer coefficient (combined convective and radiative heat

93 transfer coefficient, see section 3.2.1) (Kondjoyan and Portanguen, 2008; Sakin-Yilmazer et al.,
94 2012; Zhang and Datta, 2006). The heat is then internally transferred by conduction and
95 convection.



96
97 **Fig. 1. Schematic illustration of the main mechanisms during the roasting of chicken breast meat in a convection oven.**

98
99 Water migration within the product takes place by diffusion and convection mechanisms. The
100 latter is a result of the heat induced protein denaturation and shrinkage of the protein network,
101 which results in the decrease of the water holding capacity and a pressure gradient inside the
102 chicken meat. This so called swelling pressure is the driving force for the convective water
103 transport inside the meat and can be described by Darcy's law for flow through porous media
104 (van der Sman, 2007). Liquid water that is expelled to the product surface is then evaporated to
105 the surrounding hot air.

106 From the measured temperature profiles inside the chicken meat we observed that the
107 temperature stays below the evaporation temperature and only a thin crust is formed during the
108 roasting. Thus, internal evaporation of water was neglected in this study. Furthermore, the
109 following basic assumptions are made to formulate the governing equations for the coupled heat

110 and mass transfer: fat transport inside the chicken meat is negligible (since the fat content is less
111 than 1% in chicken breast meat), evaporated water consists of pure water (no dissolved matter,
112 measured similar to Feyissa et al. (2013)) and no internal heat generation.

113 **2.2. Governing equations**

114 **2.2.1. Heat transfer**

115 The heat transfer within the chicken breast meat is given by Eq. (1) (Bird et al., 2007)

$$116 \quad c_{p,cm} \rho_{cm} \frac{\partial T}{\partial t} = \nabla(k_{cm} \nabla T) - \rho_w c_{p,w} u_w \nabla T \quad (1)$$

117 where $c_{p,cm}$ and $c_{p,w}$ are the specific heat capacities of chicken meat and water (J/(kg K)),
118 respectively, ρ_{cm} and ρ_w are the densities of chicken meat and water (kg/m³), respectively, k_{cm} is
119 the thermal conductivity of chicken breast meat (W/(m K)), u_w the velocity of the fluid (m/s), T is
120 the temperature (K) and t is the time (s).

121 **2.2.2. Mass transfer**

122 The governing equation for water transport is based on the conservation of mass and is given by
123 Eq. (2) (Bird et al., 2007)

$$124 \quad \frac{\partial C}{\partial t} = \nabla(-D \nabla C + C u_w) \quad (2)$$

125 where C is the moisture concentration (kg of water/kg of sample) and D is the moisture diffusion
126 coefficient (m²/s).

127 Darcy's law gives the relationship between moisture transport and pressure gradient inside a
128 porous medium (in this case meat) and the velocity of the fluid inside the chicken meat can be
129 expressed as

$$130 \quad u_w = \frac{-\kappa}{\mu_w} \nabla p \quad (3)$$

131 where κ is the permeability of the chicken meat (m^2), μ_w is the dynamic viscosity of the fluid (Pa
 132 s) and ∇p is the pressure gradient vector (Pa/m). The swelling pressure is given by Eq. (4)
 133 (Barrière and Leibler, 2003; van der Sman, 2007)

$$134 \quad p = G'(C - C_{eq}) \quad (4)$$

135 with G' the storage modulus and C_{eq} the water holding capacity of chicken breast meat.

136 By inserting the expression for the swelling pressure (Eq. (4)) into Eq. (3) the following
 137 expression results for the fluid velocity u_w :

$$138 \quad u_w = \frac{-\kappa G'}{\mu_w} \nabla(C - C_{eq}) \quad (5)$$

139 The storage modulus varies with temperature and was described by with a sigmoidal function
 140 (Eq. (6)) (Rabeler and Feyissa, 2017, submitted for publication):

$$141 \quad G' = G'_{max} + \frac{(G'_0 - G'_{max})}{1 + \exp\left(\frac{T - \bar{T}}{\Delta T}\right)} \quad (6)$$

142 with $G'_{max} = 92$ kPa (the maximum value of the storage modulus for chicken meat), $G'_0 = 13.5$
 143 kPa (the initial value of the storage modulus), $\bar{T} = 69$ °C and $\Delta T = 4$ °C.

144 The change in the water holding capacity with temperature is described by Eq. (7) (van der Sman,
 145 2013):

$$146 \quad C_{eq(T)} = y_{w0} - \frac{a_1}{1 + a_2 \exp(-a_3(T - T_\sigma))} \quad (7)$$

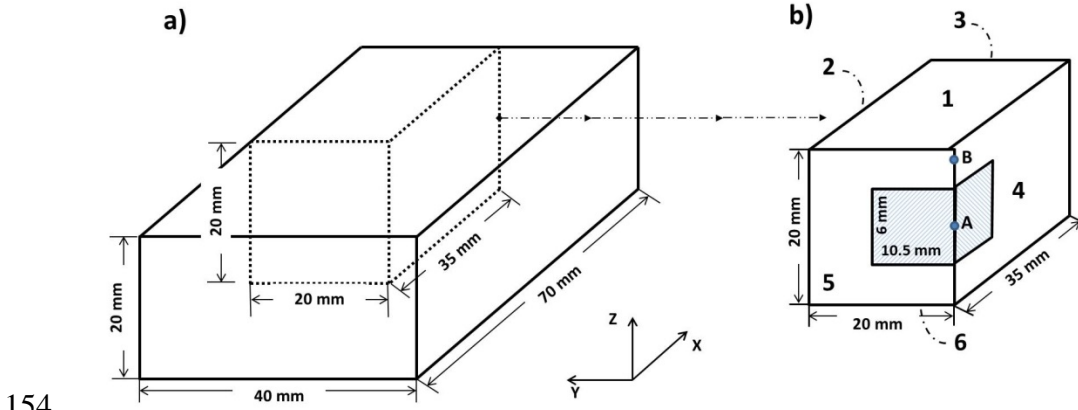
147 where $y_{w0} = 0.77$ is the initial water content of raw chicken meat, $T_\sigma = 315$ K, $a_1 = 0.31$, $a_2 = 30.0$
 148 and $a_3 = 0.17$.

149 **2.3. Initial and boundary conditions**

150 We assume a uniform initial temperature (Eq. (8)) and moisture distribution (Eq. (9)) throughout
 151 the whole sample domain (Fig. 2b):

$$152 \quad T(x, y, z, 0) = T_0 \quad (8)$$

153 $C(x, y, z, 0) = C_0$ (9)



155 Fig. 2. Schematic illustration of (a) the rectangular chicken meat sample and (b) the geometry used in the developed
 156 model. The points: A (0, 0, 10 mm) and B (0, 0, 19mm) indicate the position of the two thermocouples and the striped part
 157 shows the domain for the texture validation.

158

159 **2.3.1. Heat transfer boundary condition**

160 The boundaries 1, 2 and 3 (see Fig. 2) are exposed to the hot air and the heat flux is given by Eq.

161 (10):

162 $-k_{cm} \nabla T = h_{eff} (T_{oven} - T_{surf})$ (10)

163 where k_{cm} is the thermal conductivity of the chicken breast meat (W/(m K)), h_{eff} is the effective
 164 heat transfer coefficient (W/(m² K)), which is the sum of both the convective and radiative heat
 165 transfer (Sakin et al., 2009) (see section 3.2.1) , T_{oven} is the oven temperature (K) and T_{surf} is the
 166 surface temperature (K) of the chicken breast meat.

167 At boundary 6 the chicken meat is in contact with the roasting plate and a heat flux at this
 168 boundary is given by Eq. (11):

169 $-k_{cm} \nabla T = h_{bot} (T_{oven} - T_{bot})$ (11)

170 with the heat transfer coefficient h_{bot} and bottom surface temperature T_{bot} (W/(m² K)).

171 Boundaries 5 and 4 are symmetry boundary conditions.

172 2.3.2. Mass transfer boundary condition

173 The water evaporation at the boundaries 1, 2, 3 and 6 is given by Eq. (12):

$$174 -D \nabla C + C u_w = \beta_{tot} (C_{surf} - C_{oven}) \quad (12)$$

175 where β_{tot} is the mass transfer coefficient (m/s), C_{surf} is the water vapor concentration at the
176 surface of the meat (kg/kg) and C_{oven} the water vapor concentration in the air flow inside the
177 oven.

178 Van der Sman (2013) reported that the top layer (epimysium connective tissue) of the chicken
179 breast meat becomes glassy during the roasting which results in an increased resistance against
180 water evaporation. To take this into account the author formulated a mass transfer coefficient β_{skin}
181 (Eq. 13)) which is dependent on the local moisture content at the surface of the chicken breast
182 meat.

$$183 \beta_{skin} = \beta_1 y_w^b \quad (13)$$

184 where β_1 and b are 0.040 [m/s] and 4.0 , respectively (van der Sman, 2013).

185 The total mass transfer coefficient is then given by Eq. (14):

$$186 \frac{1}{\beta_{tot}} = \frac{1}{\beta_{ext}} + \frac{1}{\beta_{skin}} \quad (14)$$

187 where β_{ext} refers to the external mass transfer coefficient which is calculated using the Lewis
188 relation (Eq. (15)):

$$189 \beta_{ext} = \frac{h}{\rho_a c_{p,a} Le^{2/3}} \quad (15)$$

190 Boundaries 5 and 4 are symmetry boundary conditions.

191 2.4. Thermo-physical properties

192 The thermo-physical properties of chicken breast meat were described as function of composition
193 and temperature (including the effect of fiber direction) (Choi and Okos, 1986). For the thermal
194 conductivity we assume that all fibers are oriented along the x-axis (see Fig. 2) of the chicken

195 breast. The thermal conductivity parallel to the fibers ($k_{cm,\parallel}$) is calculated using the parallel
196 model (Eq. (16)) and for the thermal conductivity perpendicular to the fibers ($k_{cm,\perp}$), we assume
197 the serial model (Eq. (17)).

$$198 \quad k_{cm,\parallel} = \sum k_i \phi_i \quad (16)$$

$$199 \quad \frac{1}{k_{cm,\perp}} = \sum \frac{\phi_i}{k_i} \quad (17)$$

200 where k_i and ϕ_i are the thermal conductivities (W/(m K)) and volume fractions of the each
201 component i (water, protein, fat and ash), respectively.

202 The specific heat capacity (J/(kg K)) of chicken meat is calculated using Eq. (18)

$$203 \quad c_{p,cm} = \sum y_i c_{p,i} \quad (18)$$

204 where y_i and $c_{p,i}$ are the mass fraction and specific heat capacity of each component i (water,
205 protein, fat and ash), respectively.

206 **2.5. Kinetic model for texture changes**

207 A modified reaction rate law, which is taking into account that foods retain a non-zero
208 equilibrium even after long heating times, was used to describe the texture (hardness, gumminess
209 and chewiness) changes of chicken breast meat with temperature and time (for details see
210 (Rabeler and Feyissa, 2017, submitted for publication)) (Eq. 19):

$$211 \quad \frac{\partial Q}{\partial t} = k (Q_\infty - Q)^n \quad (19)$$

212 where Q is the quality attribute, Q_∞ is the final non-zero equilibrium quality value after long
213 heating times, k is the reaction rate constant ($\text{min}^{-1} [Q]^{1-n}$) and n the reaction order.

214 The temperature dependence of the reaction rate constant is described by the Arrhenius equation
215 as followed (Eq. (20)):

$$216 \quad k = k_0 e^{-\frac{E_a}{RT}} \quad (20)$$

217 with k_0 the pre-exponential factor ($\text{min}^{-1} [Q]^{1-n}$), E_a the activation energy in J/mol, R is the
218 universal gas constant (8.314 J/(mol K)) and T is the temperature in K.

219 The modified reaction rate law is coupled with the model for heat and mass transfer (section
220 2.4), allowing the prediction of the texture parameters hardness, gumminess and chewiness from
221 the local temperature development with time. The estimated activation energies, pre-exponential
222 factors and reaction orders by Rabeler and Feyissa, (2017, submitted for publication) were used
223 to solve Eq. (19) and (20).

224 2.6. Model solution

225 The coupled PDEs of heat and mass transfer (equations described in section 2.4) and the kinetic
226 models (ODEs) that describe the quality changes (hardness, gumminess and chewiness) (section
227 2.5) were implemented and solved using the finite element method (FEM) in the commercial
228 software, COMSOL Multiphysics 5.2a. The model input parameters are shown in Table 1. A
229 rectangular geometry with the dimensions illustrated in Fig. 2b was built in COMSOL and
230 meshed. Mesh sensitivity analysis was conducted, where the mesh size was decreased in a series
231 of simulations until it had no further impact on the model solution (Kumar and Dilber, 2006).

232

233 **Table 1: Model input parameters**

Parameter	Symbol	Value	Unit	Source
Density				
chicken meat	ρ_{cm}	1050	kg/m ³	Calculated from (Choi and Okos, 1986)
water	ρ_w	998	kg/m ³	
Diffusion coefficient	D	3×10^{-10}	m ² /s	(Ngadi et al., 2006)
Permeability	κ	3×10^{-17}	m ²	(Datta, 2006)

Viscosity water	μ_w	0.988×10^{-3}	Pa s	
Initial composition				
Water	y_{w0}	0.76	kg/kg	Measured
Protein	y_{p0}	0.22	kg/kg	(Barbanti and Pasquini, 2005)
Fat	y_{f0}	0.01	kg/kg	(Barbanti and Pasquini, 2005)
Ash	y_{a0}	0.01	kg/kg	(Barbanti and Pasquini, 2005)
Latent heat of vaporization of water	H_{evap}	2.3×10^6	J/kg	
Initial meat temperature	T_0	6	°C	Measured
Initial moisture concentration	C_0	0.76	kg/kg	Measured
Water vapor concentration in ambient air	C_{air}	0.05	kg/kg	Measured
Heat transfer coefficient				
High fan speed	h_{eff}	44	W/(m ² K)	Measured
	h_{bot}	59	W/(m ² K)	
Low fan speed	h_{eff}	21	W/(m ² K)	Measured
	h_{bot}	41	W/(m ² K)	

234

235 3. Materials and Methods

236 3.1. Sample preparation and oven settings

237 Chicken breast meat (skinless and boneless) was purchased from a local supermarket the same
238 day as the experiments and stored in plastic bags at 4 °C until it was used. For all roasting
239 experiments, the chicken breasts were cut into rectangular blocks with the dimensions of 0.04 m
240 x 0.02 m x 0.07 m and a weight of $63 \text{ g} \pm 2 \text{ g}$. The fiber direction for all samples was along the x-
241 axis (see Fig. 2).

242 A professional convection oven with roasting chamber dimensions of 0.45 m x 0.50 m x 0.65 m
243 was used for the roasting experiments. Dry hot air was circulated inside the roasting chamber by
244 a fan, while the fan speed (air speed) could be adjusted. The oven temperature was controlled by
245 the oven thermostat and additionally two thermocouples were placed at different positions in the
246 oven to measure the oven temperature continuously. The measured oven temperature was stable
247 around the set point with a standard deviation of ± 3 °C. Before each experimental run, the oven
248 was preheated to the desired temperature for 30 min to ensure steady state conditions. The
249 following process settings were used to show the effect of process conditions on the temperature,
250 moisture and texture profile and to validate the developed model:

251 Setting I: $T_{oven} = 170$ °C, high fan speed (HF)

252 Setting II: $T_{oven} = 230$ °C, high fan speed (HF)

253 Setting III: $T_{oven} = 230$ °C, low fan speed (LF)

254 **3.2. Experimental data**

255 **3.2.1. Heat transfer coefficient**

256 The combined heat transfer coefficient, which is the sum of the radiative and convective heat
257 transfer coefficient, was estimated using the lumped method (Sakin et al., 2009). The oven was
258 preheated for 30 min before the experiments to ensure steady state conditions. Polished silver and
259 black painted aluminum blocks (rectangular) were placed in the oven and heated for 20 min at
260 200 °C. The temperature in the center of the blocks was recorded continuously by using a
261 thermocouple. As the Biot number was smaller than 0.1 the lumped heat transfer method was
262 used and the combined heat transfer coefficient estimated as described by Feyissa et al. (2013).
263 Only minor differences (less than 5%) between the estimated heat transfer coefficients for the
264 black and polished aluminum block was found. This means that the radiative heat transfer from

265 the oven walls is small compared to the convective heat transfer. Furthermore, the heat flux by
266 radiation (assuming $T_{oven} = 200\text{ °C}$, $\varepsilon_{chicken} = 0.8$, $T_{surf} = 100\text{ °C}$) is small ($\approx 2\%$ of the total flux)
267 compared to the convective heat flux. In the model the estimated effective heat transfer
268 coefficient, which includes the radiative effect, was used as described by Kondjoyan and
269 Portanguen (2008), Sakin-Yilmazer et al. (2012) or Zhang and Datta (2006).

270 **3.2.2. Local temperature**

271 In order to measure the temperature profile inside the chicken meat sample, two thermocouples
272 were placed at the center (point A, Fig. 2b)) and close to surface (point B, Fig. 2b) of the sample.
273 One sample was then placed centrally on the roasting tray and the tray positioned in the middle of
274 the oven. The temperature development was measured as function of time with sample intervals
275 of 5 seconds for 15 min (for setting II, see section 3.1) and 20 min (for setting I and III).

276 **3.2.3. Moisture content**

277 To compare the predicted and measured moisture content at different time steps, roasting
278 experiments were performed with different times: 1, 3, 5, 7, 10 and 15 min for all process
279 settings. For setting I and III (see section 3.1), an additional sample was taken at 20 min of
280 roasting. The samples were taken out of the oven after the corresponding roasting time, sealed in
281 plastic bags and placed in ice water to stop further water loss from the surface. The average
282 moisture content of the whole chicken meat sample was then measured using the oven drying
283 method (Bradley, 2010). The samples were minced, weighed in aluminum cups and dried for 24
284 hours at 105 °C . From the weight difference before and after the drying, the moisture content of
285 the chicken meat samples was calculated.

286 **3.2.4. Texture measurements**

287 To validate the predicted texture development, roasting experiments were conducted at different
288 time steps: 3, 5, 7, 10, 15 and 20 min (20 min only for Settings I and III, see section 3.1). After
289 the roasting process, the samples were immediately placed in ice water for 4 min to cool them
290 down quickly. The samples were then stored at room temperature for 2 hours in sealed aluminum
291 cups before the texture measurements.

292 To measure the textural changes of chicken breast meat, double compression tests (TPA) were
293 performed according to the procedure described by Rabeler and Feyissa (2017, submitted for
294 publication). A cylindrical probe with a height of 6 mm \pm 0.5 and a diameter of 21 mm \pm 1 was
295 cut out of the middle of the roasted chicken samples using a cork borer. The same sample
296 dimension as in Rabeler and Feyissa (2017, submitted for publication) were used for the TPA
297 measurements. The samples were compressed to a final strain of 40 %, setting the test speed to 1
298 mm/s with time interval of 5s between the first and second stroke. The TPA parameters hardness,
299 gumminess and chewiness were then calculated from the recorded force-time plot (Bourne,
300 2002).

301 **3.3. Statistical analysis**

302 The chi-square test was used to evaluate the goodness-of-fit between the model predictions and
303 the experimental data for the temperature, moisture and texture (Eq. 21) (Taylor, 1997):

$$304 \chi^2 = \sum_{i=1}^n \frac{(\hat{\theta}_i - \theta_i)^2}{\sigma_i^2} \quad (21)$$

305 with $\hat{\theta}$ the predicted value, θ the measured value and σ the standard deviation. A significance
306 level of $P < 0.05$ was used.

307 Furthermore, the root mean squared error (RMSE) was calculated by using Eq. (22):

$$308 RMSE = \sqrt{\frac{\sum_{i=1}^n (\hat{\theta}_i - \theta_i)^2}{n}} \quad (22)$$

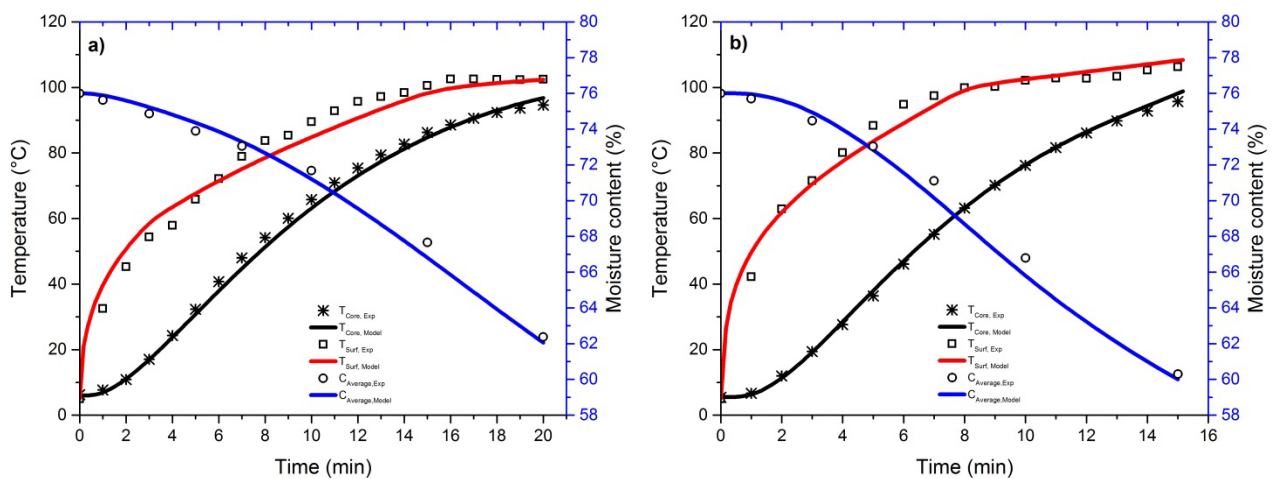
309 where n is the total number of samples.

310 4. Results and discussion

311 4.1. Temperature and moisture predictions

312 Fig. 3 presents the predicted core (at position A, Fig. 2b) and surface (at position B. Fig. 2b)
313 temperature as well as the predicted average moisture content as function of the roasting time for
314 the different process settings (Fig.3a for setting I, Fig. 3b for setting II, and Fig. 3c for setting
315 III). A good agreement between the measured (symbols) and predicted (solid lines) temperature
316 profiles at the core ($RMSE = 1.85, 0.83$ and 0.99 °C for setting I, II and III, respectively) and
317 close to the surface ($RMSE = 3.76, 2.69$ and 2.6 °C for setting I, II and III, respectively) was
318 found for all tested process settings. Furthermore, the model showed a high accuracy in the
319 prediction of the average moisture content development of the chicken meat sample with $RMSE$
320 values of $1.15, 1.39$ and 0.91 % for setting I, II and III, respectively ($\chi^2 = 4.78, 4.66$ and $3.97,$
321 respectively, $P > 0.05$) (see also Fig. 3a to 3c).

322



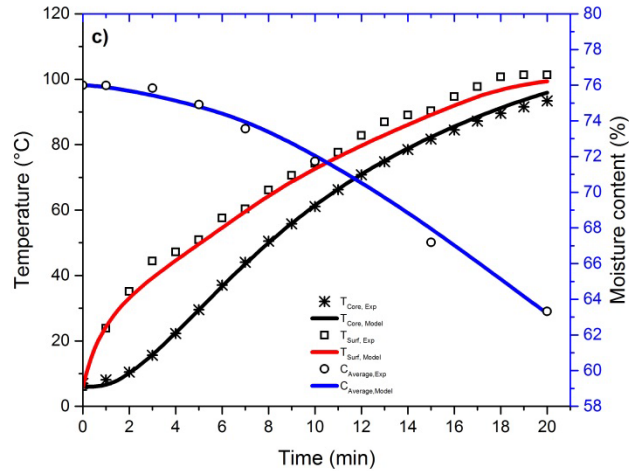


Fig. 3. Comparison between the predicted and measured temperature (core and surface) and moisture development of the chicken meat sample with varying air temperature and fan speed: a) Setting I: $T_{oven} = 170\text{ }^{\circ}\text{C}$, high fan speed; b) Setting II: $T_{oven} = 230\text{ }^{\circ}\text{C}$, high fan speed; c) Setting III: $T_{oven} = 230\text{ }^{\circ}\text{C}$, low fan speed.

323

324 The process conditions have an influence on the temperature and moisture content profile during

325 the roasting process. Chicken breast meat should be heated to a core (coldest point) temperature

326 of $75\text{ }^{\circ}\text{C}$ to ensure a safe product for the consumers (Fsis, 2000). The time needed to reach this

327 temperature in the core varies with the process settings: 12.5 min, 10 min and 13 min roasting

328 time for setting I ($T_{oven} = 170\text{ }^{\circ}\text{C}$ and high fan speed, Fig. 3a), setting II ($T_{oven} = 230\text{ }^{\circ}\text{C}$ and high

329 fan speed, Fig. 3b) and setting III ($T_{oven} = 230\text{ }^{\circ}\text{C}$ and low fan speed, Fig. 3c), respectively.

330 The higher temperature and fan speed for setting II compared to setting I and III, respectively,

331 leads to an increased heat flux from the surrounding hot air to the sample surface. Consequently,

332 the surface temperature is rising faster, which also leads to a faster increase of the core

333 temperature. However, the high surface temperature for setting II results in an increased

334 evaporation of moisture from the chicken meat surface. Therefore, a lower average moisture

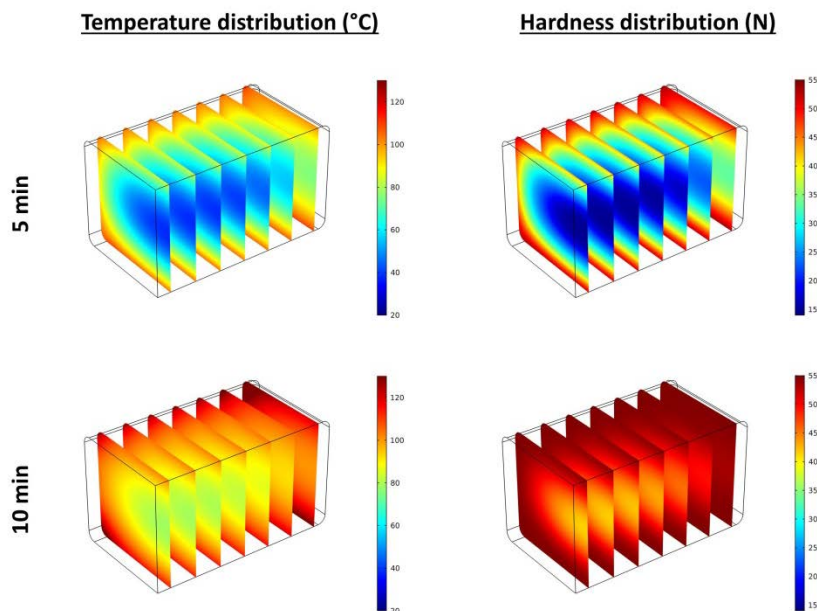
335 content is reached for setting II ($C_{av}(t=10\text{min}) \approx 66\%$, Fig. 3b) compared to setting I ($C_{av}(t$

336 $=12.5\text{min}) \approx 69\%$, Fig. 3a) and setting III ($C_{av}(t_{75^{\circ}\text{C}}=13\text{min}) \approx 70\%$).

337 Setting I and III show a similar temperature and moisture content development with roasting time
338 (Fig. 3a and 3c, respectively). This is reasonable as the heat flux from the surrounding hot air to
339 the chicken meat surface is comparable for the two settings ($\dot{q} = 3080, 5720$ and 2730 W/m^2 for
340 setting I, II and III, respectively) (see Eq. 12 and 13). Thus, the times to reach $75 \text{ }^\circ\text{C}$ in the core
341 as well as the moisture contents at this time step are comparable.

342 4.2. Prediction of texture changes

343 By coupling the model for heat and mass transfer with the kinetics for textural changes, it is
344 possible to predict the spatial and local texture change inside the chicken meat from the local
345 temperature development. Fig. 4 presents the simulated temperature and texture distributions
346 inside the chicken meat during the roasting in the convection oven (for setting II, $T_{oven} = 230 \text{ }^\circ\text{C}$
347 and high fan speed) for 5 min (Fig. 4a and 4c) and 10 min (Fig 4b and Fig. 4d).



348 Fig. 4. Visualization of the simulated temperature and hardness distribution during the roasting process: a)
349 temperature profile at $t = 5 \text{ min}$; b) temperature profile at $t = 10 \text{ min}$; c) hardness profile at $t = 5 \text{ min}$; d)
hardness profile at $t = 10 \text{ min}$. Setting II: $T_{oven} = 230 \text{ }^\circ\text{C}$, high fan speed.

350 The results illustrate that the development of the texture parameter hardness, but also the
351 development of the other studied texture parameters (gumminess and chewiness, not shown
352 here), is following the temperature changes. The high heat flux from the surrounding hot air is
353 leading to a fast temperature increase of the chicken meat surface (see also Fig. 3b). This
354 subsequently, results in a fast hardening of the chicken meat at the surface. On the contrary, the
355 internal heat transfer is slow ($Bi = 1.1 > 0.1$), which leads to a delayed heat up towards the center
356 of the chicken meat. Accordingly, the hardness at the center is changing slower compared to the
357 surface.

358 Overall, it becomes obvious that the non-uniform temperature development of the chicken meat
359 sample results in the non-uniform texture profiles. The developed model is, therefore, a strong
360 tool to predict the spatial texture development as function of the process conditions and roasting
361 time which is difficult or even not possible to obtain by experimentation alone.

362 **4.3. Effect of process parameters on the texture profile and model validation**

363 In order to study the influence of the oven settings on the texture development of chicken breast
364 meat and to validate the developed model, simulations with two different oven temperatures (230
365 °C and 170 °C) and fan speeds were compared (see process settings in section 3.1). The
366 predictions of the texture development with roasting time were validated against experimental
367 values that were obtained according to section 3.2.4. Fig. 5a to 5c show that a good agreement
368 between the predicted (solid lines) and experimental measured texture changes (hardness,
369 gumminess and chewiness) (symbols) of chicken breast meat was found for all tested process
370 settings. The *RMSE* and χ^2 values for hardness, gumminess and chewiness are summarized in
371 Table 2. The results further show that the model is able to accurately predict the texture changes
372 of chicken breast meat during roasting for all tested process settings.

373

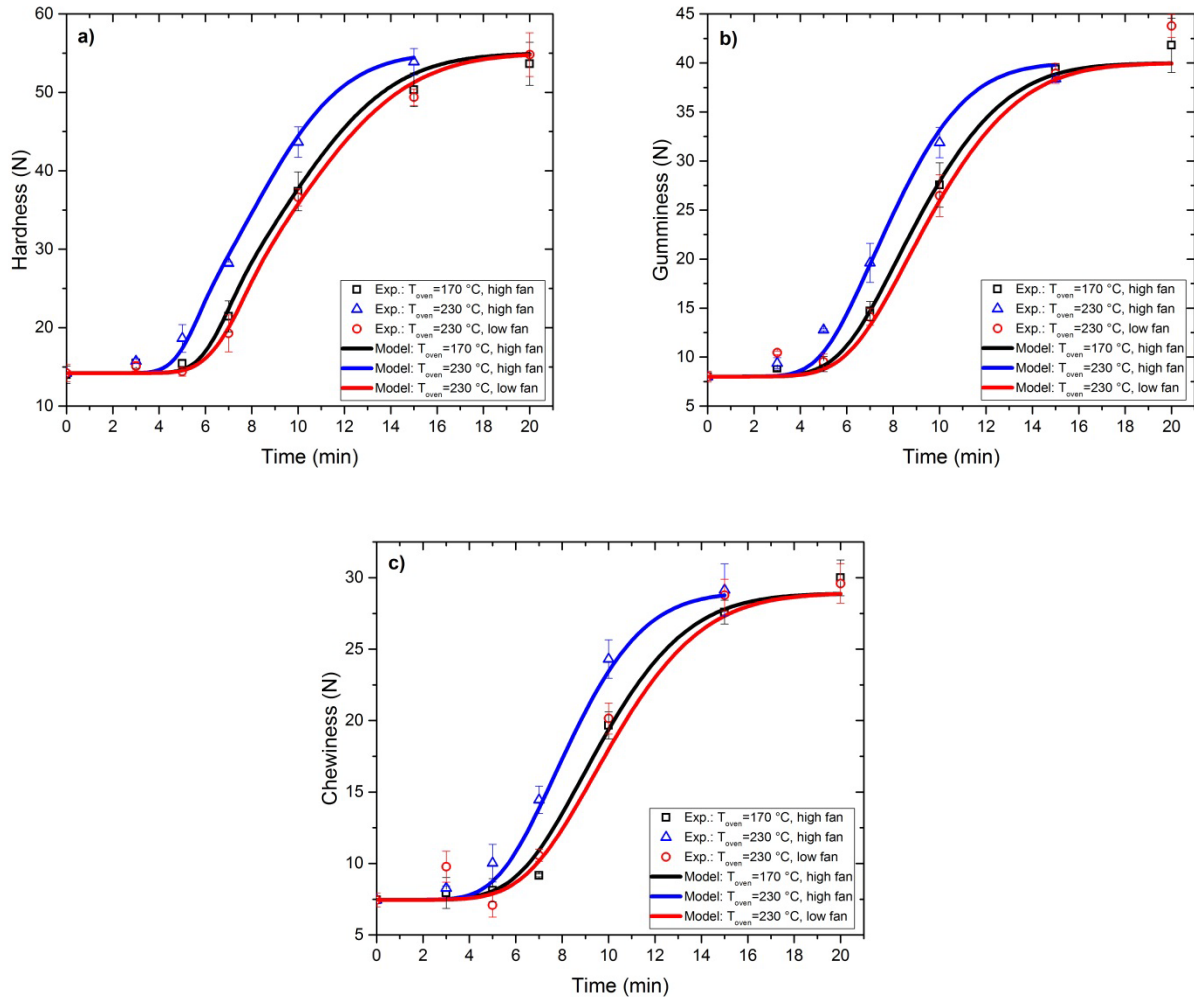


Fig. 5. Effect of process settings on the texture changes of chicken breast meat and comparison between predicted (lines) and experimental values (symbols): a) hardness (N), b) gumminess, c) chewiness. Bars indicate the standard deviation (n = 3).

374

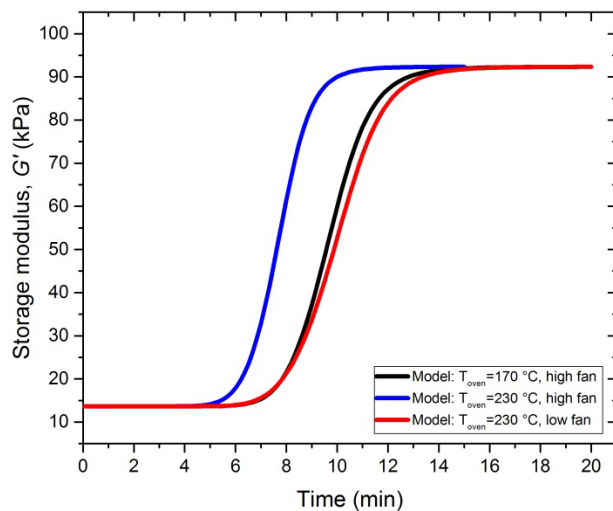
375 Table 2: RMSE and χ^2 values for hardness, gumminess and chewiness for process setting I, II, and III.

	Hardness		Gumminess		Chewiness	
	<i>RMSE</i>	χ^2	<i>RMSE</i>	χ^2	<i>RMSE</i>	χ^2
Setting I	2.06 N	7.12	1.79 N	2.35	2.12 N	7.50
Setting II	1.70 N	2.90	2.11 N	5.12	2.11 N	3.63
Setting III	2.25 N	6.20	2.08 N	6.33	2.73 N	7.17

376

377 The oven temperature has a high influence on the texture (hardness, gumminess and chewiness)
378 profiles (Fig. 5a to 5c). A higher value of T_{oven} leads to an increased heat flux from the
379 surrounding hot air to the chicken meat surface (see Eq. (10) and Eq. (11)) which results in a
380 faster heat up of the sample (see also Fig. 3a and 3b). Therefore, the texture parameters (that are a
381 function of the local temperature development with time) start to rise earlier for the oven
382 temperature of 230 °C (red line) compared to 170 °C (black line) (setting II and I, respectively).
383 A higher fan speed results in a higher heat transfer coefficient (h_{eff} and h_{bot} , see Table 1) which
384 leads to an increased heat flux to the chicken meat surface (see Eq. (10) and Eq. (11)).
385 Accordingly, the texture parameter rise earlier for the high fan speed (black lines, Fig. 4)
386 compared to the low fan speed (blue lines).
387 However, only a slight difference in the predicted profiles for hardness, gumminess and
388 chewiness was found between the oven settings I and III (see section 3.1). This is reasonable as a
389 similar temperature development of the two different oven settings was found (compare Fig. 3a
390 with 3c), which results in the similar texture changes.
391 The predicted changes of the storage modulus with heating time for the tested process settings are
392 presented in Fig. 6. A similar trend between the storage modulus and the TPA parameters
393 hardness, gumminess and chewiness development with time was found for all tested process
394 settings (compare Fig. 6 with Fig. 5a – 5c). Setting II (230 °C, high fan speed) leads to an earlier
395 rise of the storage modulus compared to the lower oven temperature (setting I) and lower fan
396 speed (setting III). Similar to the TPA parameters development only slight differences in the
397 storage modulus development was observed between setting I and III (see Fig. 6). However, we
398 found that the storage modulus starts to rise later (around 55 °C) compared to the texture
399 parameters hardness, gumminess and chewiness (around 45 °C) (compare Fig. 6 with Fig. 5a –
400 5c). This earlier increase of the TPA parameters could be due to the earlier decrease of the water

401 holding capacity at around 40 °C which leads to a water release into the pore spaces between the
402 meat fibers (Micklander et al., 2002; van der Sman, 2013). Consequently, parts of the
403 compression energy (TPA measurements) could be dissipated as a result of the viscous flow of
404 the fluid in the pore space which results in a toughening of the meat (Tornberg, 2005) . However,
405 deeper analyses of the heat induced changes in the microstructure of chicken breast meat are
406 necessary to obtain a clear relationship between the storage modulus and the TPA parameters
407 hardness, gumminess and chewiness.



408
409 **Fig. 6. Predicted storage modulus (G') development with time for the oven settings I (black line), II (blue line) and III (red**
410 **line).**

411
412 Overall, the results show that by adjusting the oven settings, the texture of the chicken meat
413 sample can be influenced. Consequently, the developed model can be used to control the quality
414 (texture) of the product and to optimize the roasting process to obtain a safe final product with the
415 highest quality for the consumer.

416 **Conclusion**

417 In this study, a mechanistic model of heat and mass transfer was developed for the roasting of
418 chicken breast meat in a convection oven. The developed model was then coupled with the
419 kinetics for heat induced texture changes. This enabled the prediction of the spatial and local
420 texture development as function of the process parameters. The simulation results were validated
421 against experimental obtained values. The developed model provides a more detailed
422 understanding of the process mechanisms during roasting chicken breast meat.

423 We showed that the non-uniform temperature distribution inside the chicken meat sample during
424 the roasting process, leads to a non-uniform texture profile. Furthermore, the clear effect of
425 changing roasting parameters on the texture development was obtained. The developed model
426 enables, thus, a deep insight into the effects of the process conditions on the texture changes of
427 chicken breast meat that is difficult or even not possible to obtain by experimentation alone.

428

a_w	water activity	Greek symbols	
C	mass concentration (kg/kg)	α	pre-factor (-)
c_p	specific heat capacity (J/(kg K))	β	mass transfer coefficient (m/s)
C_w	chewiness	κ	permeability (m ²)
D	diffusion coefficient (m ² /s)	μ	dynamic viscosity (Pa s)
E_a	activation energy (J/mol)	ρ	density (kg/m ³)
G'	storage modulus (Pa)	ϕ	volume fraction
Gu	Gumminess	$\hat{\theta}_i$	predicted value (T, C, Ha, Gu, C_w)
h	heat transfer coefficient (W/(m ² K))	θ_i	measured value (T, C, Ha, Gu, C_w)
Ha	hardness (N)	σ	standard deviation
k	reaction rate constant (1/min)	χ^2	chi-square value
k_0	pre-exponential factor (1/min)	Subscripts	
k_i	thermal conductivity (W/(m K))	a, f, p, w	ash, fat, protein, water
M_w	molar weight of water (0.018 kg/mol)	bot	bottom
n	number of samples	cm	chicken meat
p	swelling pressure (Pa)	eff	effective
Q	quality attribute	eq	equilibrium
R	universal gas constant (8.314 J/mol K)	ext	external
T	temperature (K)	surf	surface
t	time (s)	sat	saturation
u	velocity (m/s)	tot	total
y	mass fraction	0	initial (t=0)
TPA	texture profile analyses		
Bi	Biot number		
RMSE	Root-mean-squared-error		

432 **References**

- 433 Barbanti, D., Pasquini, M., 2005. Influence of cooking conditions on cooking loss and tenderness
434 of raw and marinated chicken breast meat. *LWT - Food Sci. Technol.* 38, 895–901.
435 doi:10.1016/j.lwt.2004.08.017
- 436 Barrière, B., Leibler, L., 2003. Kinetics of solvent absorption and permeation through a highly
437 swellable elastomeric network. *J. Polym. Sci. Part B Polym. Phys.* 41, 166–182.
438 doi:10.1002/polb.10341
- 439 Bird, R.B., Stewart, W.E., Lightfoot, E.N., 2007. *Transport Phenomena, Revised 2n. ed.* John
440 Wiley & Sons, Inc.
- 441 Bourne, M.C., 2002. *Principles of Objective Texture Measurement. Food Texture Viscosity
442 Concept Meas. 2nd Ed.*
- 443 Bradley, R.L.J., 2010. Food Analysis, in: Nielsen, S.S. (Ed.), *Food Analysis S.* Springer-Verlag,
444 West Lafayette, IN, USA, pp. 85–104.
- 445 Chang, H.C., Carpenter, J.A., Toledo, R.T., 1998. Modeling Heat Transfer During Oven Roasting
446 of Unstuffed Turkeys. *J. Food Sci.* 63, 257–261. doi:10.1111/j.1365-2621.1998.tb15721.x
- 447 Chen, H., Marks, B.P., Murphy, R.Y., 1999. Modeling coupled heat and mass transfer for
448 convection cooking of chicken patties. *J. Food Eng.* 42, 139–146. doi:10.1016/S0260-
449 8774(99)00111-9
- 450 Choi, Y., Okos, M.R., 1986. Effects of temperature and composition on the thermal properties of
451 foods. *Food Eng. Process Appl.* 93–101.
- 452 Christensen, M., Purslow, P.P., Larsen, L.M., 2000. The effect of cooking temperature on
453 mechanical properties of whole meat, single muscle fibres and perimysial connective tissue.
454 *Meat Sci.* 55, 301–307. doi:10.1016/S0309-1740(99)00157-6
- 455 Datta, A.K., 2006. Hydraulic Permeability of Food Tissues. *Int. J. Food Prop.* 9, 767–780.

456 doi:10.1080/10942910600596167

457 Feyissa, A.H., Gernaey, K. V., Adler-Nissen, J., 2013. 3D modelling of coupled mass and heat
458 transfer of a convection-oven roasting process. *Meat Sci.* 93, 810–820.
459 doi:10.1016/j.meatsci.2012.12.003

460 Fletcher, D.L., Qiao, M., Smith, D.P., 2000. The relationship of raw broiler breast meat color and
461 pH to cooked meat color and pH. *Poult. Sci.* 79, 784–788. doi:10.1093/ps/79.5.784

462 Fsis, U., 2000. *Chicken from Farm to Table* 1–8.

463 Guerrero-Legarreta, I., Hui, Y.H., 2010. *Handbook of Poultry Science and Technology, Volume*
464 *2: ed. John Wiley & Sons, Inc.* doi:10.1002/9780470504475

465 Huang, E., Mittal, G.S., 1995. Meatball cooking - modeling and simulation. *J. Food Eng.* 24, 87–
466 100. doi:10.1016/0260-8774(94)P1610-A

467 Isleroglu, H., Kaymak-Ertekin, F., 2016. Modelling of heat and mass transfer during cooking in
468 steam-assisted hybrid oven. *J. Food Eng.* doi:10.1016/j.jfoodeng.2016.02.027

469 Kassama, L.S., Ngadi, M.O., Campus, M., 2014. Pore Development and Moisture Transfer in
470 Chicken Meat during Deep-Fat Frying. *Dry. Technol.* 3937. doi:10.1081/DRT-200054239

471 Kondjoyan, A., Oillic, S., Portanguen, S., Gros, J.B., 2013. Combined heat transfer and kinetic
472 models to predict cooking loss during heat treatment of beef meat. *Meat Sci.* 95, 336–344.
473 doi:10.1016/j.meatsci.2013.04.061

474 Kondjoyan, A., Portanguen, S., 2008. Prediction of surface and “under surface” temperatures on
475 poultry muscles and poultry skins subjected to jets of superheated steam. *Food Res. Int.* 41,
476 16–30. doi:10.1016/j.foodres.2007.07.006

477 Kumar, A., Dilber, I., 2006. *Fluid Flow and Its Modeling Using Computational Fluid Dynamics,*
478 *in: Sablani, S., Datta, A., Shafiur Rehman, M., Mujumdar, A. (Eds.), Handbook of Food and*
479 *Bioprocess Modeling Techniques, Food Science and Technology. CRC Press.*

480 doi:10.1201/9781420015072

481 Lawrie, R.A., Ledward, D.A., 2006. Lawrie's meat science.

482 Lewis, G.J., Purslow, P.P., 1989. The strength and stiffness of perimysial connective tissue
483 isolated from cooked beef muscle. *Meat Sci.* 26, 255–269. doi:10.1016/0309-
484 1740(89)90011-9

485 Micklander, E., Peshlov, B., Purslow, P.P., Engelsen, S.B., 2002. NMR-cooking: Monitoring the
486 changes in meat during cooking by low-field ¹H-NMR. *Trends Food Sci. Technol.* 13, 341–
487 346. doi:10.1016/S0924-2244(02)00163-2

488 Ngadi, M., Dirani, K., Oluka, S., 2006. Mass Transfer Characteristics of Chicken Nuggets. *Int. J.*
489 *Food Eng.* 2. doi:10.2202/1556-3758.1071

490 Obuz, E., Powell, T.H., Dikeman, M.E., 2002. Simulation of Cooking Cylindrical Beef Roasts.
491 *LWT - Food Sci. Technol.* 35, 637–644. doi:10.1006/fstl.2002.0940

492 Rabeler, F., Feyissa, A.H., 2017. Kinetic modelling of texture and color changes during thermal
493 treatment of chicken breast meat, (manuscript submitted for publication).

494 Sakin-Yilmazer, M., Kaymak-Ertekin, F., Ilicali, C., 2012. Modeling of simultaneous heat and
495 mass transfer during convective oven ring cake baking. *J. Food Eng.* 111, 289–298.
496 doi:10.1016/j.jfoodeng.2012.02.020

497 Sakin, M., Kaymak-Ertekin, F., Ilicali, C., 2009. Convection and radiation combined surface heat
498 transfer coefficient in baking ovens. *J. Food Eng.* 94, 344–349.
499 doi:10.1016/j.jfoodeng.2009.03.027

500 Taylor, J.R., 1997. An introduction to error analysis: the study of uncertainties in physical
501 measurements, 2nd edition. University Science Books.

502 Thussu, S., Datta, A.K., 2012. Texture prediction during deep frying: A mechanistic approach. *J.*
503 *Food Eng.* 108, 111–121. doi:10.1016/j.jfoodeng.2011.07.017

504 Tornberg, E., 2005. Effects of heat on meat proteins - Implications on structure and quality of
505 meat products. *Meat Sci.* 70, 493–508. doi:10.1016/j.meatsci.2004.11.021

506 van der Sman, R.G.M., 2013. Modeling cooking of chicken meat in industrial tunnel ovens with
507 the Flory-Rehner theory. *Meat Sci.* 95, 940–957. doi:10.1016/j.meatsci.2013.03.027

508 van der Sman, R.G.M., 2007. Moisture transport during cooking of meat: An analysis based on
509 Flory-Rehner theory. *Meat Sci.* 76, 730–738. doi:10.1016/j.meatsci.2007.02.014

510 Wattanachant, S., Benjakul, S., Ledward, D.A., 2005. Effect of heat treatment on changes in
511 texture, structure and properties of Thai indigenous chicken muscle. *Food Chem.* 93, 337–
512 348. doi:10.1016/j.foodchem.2004.09.032

513 Zell, M., Lyng, J.G., Cronin, D.A., Morgan, D.J., 2010. Ohmic cooking of whole turkey meat -
514 Effect of rapid ohmic heating on selected product parameters. *Food Chem.* 120, 724–729.
515 doi:10.1016/j.foodchem.2009.10.069

516 Zhang, J., Datta, A.K., 2006. Mathematical modeling of bread baking process. *J. Food Eng.* 75,
517 78–89. doi:10.1016/j.jfoodeng.2005.03.058

518